

Electrochemical sensor based on molecularly imprinted membranes at Au@CNTs nanocomposite-modified electrode for determination of prednisolone as a doping agent in sport

Wenhong Wang

Department of Physical Education, Jinling Institute of Technology, Nanjing, 211169, China

*E-mail: wwh@jit.edu.cn

Received: 24 October 2021 / Accepted: 29 November 2021 / Published: 5 January 2022

This study was performed on fabrication of electrochemical sensors based on molecularly imprinted membranes at Au@CNTs nanocomposite-modified electrode for determination of prednisolone (PNS) as a sports doping agent. The Au@CNTs composite was deposited on GCE surface, and *p*-aminothiophenol and tetrabutylammonium perchlorate were electropolymerized on Au@CNTs/GCE. Studies on the morphology and microstructure of modified electrodes by SEM and XRD showed that Au nanoparticles were homogeneously deposited on porous network of CNTs in Au@CNTs nanocomposite, and porous structure of MIP/Au@CNTs/GCE confirming the successful electropolymerization MIP and removal of 2-oxindole template from the body of polymer network. The electrochemical analyses using the CV, DPV and amperometry indicated stable, sensitive and selective performance of MIP/Au@CNTs/GCE to determine PNS. The detection limit, sensitivity and linear range of proposed sensor were found of 0.003 μ M, 0.86207 μ A/ μ M and 1-210 μ M, respectively, and comparison between the sensing properties of sensor in this work with the reported PNS sensors in literatures demonstrated a wide linear range and a lower detection limit of MIP/Au@CNTs/GCE as PNS sensor that was attributed to the synergistic catalytic effect of MIP and Au@CNTs nanocomposite. The validity and accuracy of MIP/Au@CNTs/GCE for determination of PNS were examined in prepared specimens of blood serum 5 young athletes aged 19 to 23 years who used PNS tablet and the results for determination of PNS in each sample through the amperometry and ELISA techniques indicated to good precision (RSD less than 4.15%) and good agreement between the ELISA and amperometry measurement on MIP/Au@CNTs/GCE. Therefore, MIP/Au@CNTs/GCE as a reliable PNS sensor may be used to monitor PNS level in blood serum of athletes.

Keywords: Molecularly imprinted polymers; CNTs; Au nanoparticles; Prednisolone; doping agent; blood serum; Amperometry

1. INTRODUCTION

Glucocorticoids are essential steroid hormones secreted from the adrenal gland in response to stress and play significant roles in metabolism and inflammation [1, 2]. These steroid hormones are

major components in immunosuppressive treatments for solid organ transplantation. Prednisolone (PNS, (8S,9S,10R,11S,13S,14S,17R)-11,17-dihydroxy-17-(2-hydroxyacetyl)-10,13-dimethyl-7,8,9,11,12,14,15,16-octahydro-6H-cyclopenta[a]phenanthren-3-one) is a corticosteroid that is used to treat many different conditions such as hormonal disorders, allergic disorders, kidney disorders, ulcerative colitis, psoriasis, blood cell disorders and arthritis [3, 4].

Molecules of PNS diffuse across cell membranes and bind to glucocorticoid receptors, thereby the receptor-glucocorticoid complexes can able to move into the cell nucleus where dimerize via their DNA binding domain and bind to glucocorticoid response elements [5-7]. It inhibits proinflammatory signals, and promotes anti-inflammatory signals. Therefore, PNS modifies the immune response of the human body to various medical conditions [8]. The most common side effects of prednisolone are insomnia, weight gain, indigestion and sweating a lot [9].

However, PNS and other glucocorticosteroids are banned by the World Anti-Doping Agency [10]. Injection or oral administration of PNS into muscle reduces the pain and inflammation that often occurs with extreme exertion [11, 12]. Athletes have reported that glucocorticosteroids help them push through the pain of extreme exertion and allow them to recover faster for the next event [13, 14]. Short-term PNS intake can considerably improve performance during submaximal exercise. Therefore, it can eliminate the opportunity for fair competition. Therefore, many studies have been focused on determination PNS in clinical samples and human body fluids using liquid chromatography [15], mass spectrometry [16], gas chromatography [17], ultraviolet detection [18], fluorogenic DNA Probes [19], fourier transform Raman spectroscopy [20], and electrochemical methods [21-23]. Between these methods, electrochemical techniques have been developed as a simple, low cost and sensitive method for clinical diagnostics, food industries and environmental monitoring [24, 25]. The stability, selectivity and sensitivity of electrochemical sensors can be enhanced by modification of electrodes with a wide range of nanostructures, bio-recognition elements and compositions. Thus, this study performed synthesis of electrochemical sensors based on MIP/Au@CNTs to determine PNS as a doping agent in sport.

2. EXPERIMENTAL

Prior modification the GCE, the GCE surface was polished with alumina slurries (0.3 μm , Meck, Germany) on a polishing cloth (LAM PLAN S.A., Gaillard, France) for 15 minutes, and then cleaned in an ultrasonic bath for 6 minutes, and then rinsed with deionized water. The 5g CNTs ($\geq 70\%$, Sigma-Aldrich) was dispersed in 0.5 $\text{HAuCl}_4 \cdot 3\text{H}_2\text{O}$ ($\geq 99.9\%$, Sigma-Aldrich) aqueous solution containing 0.1 M H_2SO_4 (). The resulting mixture was treated at potential of -0.15 V constantly for 6 minutes. Electrodeposition of Au@CNTs nanocomposite was carried out using Autolab potentiostat-galvanostat (PGSTAT. 101 and PGSTAT 128N, Ecochemie, Utrecht, Netherlands) in the electrochemical cell contained an Ag/AgCl reference electrode (3 M KCl), Pt disc as the auxiliary electrodes, and GCE as a working electrode. Electrodeposition conducted on cyclic voltammetry (CV) technique at a potential range from -1.3 to 1.3 V at a scan rate of 15 mV/s for 20 cycles [26]. After electrodeposition, the Au@CNTs/GCE was immersed for 60 minutes in the solution

which prepared from ethanol (99%, Sino-Ally International Trade Co., Ltd., China), 50 mM ρ -aminothiophenol (ρ -ATP, $\geq 97.0\%$, Sigma-Aldrich), 50 mM tetrabutylammonium perchlorate (TBAP, $\geq 98.0\%$, Sigma-Aldrich) and 10mM 2-oxindole (97.0%, Sigma-Aldrich). Then, electropolymerization was performed using CV technique at potential range from -0.4 to 1.3 V at a scan rate of 15mV/s for 20 cycles [27]. After that, to remove the 2-oxindole template and form the specific holes in the membrane, the electropolymerized nanocomposite was rinsed with $1\text{M H}_2\text{SO}_4$ for 5 minutes. Finally, the resulted MIP/Au@CNTs/GCE were rinsed with a mixture of deionized water and ethanol.

Blood serum samples of 5 young athletes aged 19 to 23 years were provided who used a PNS tablet which contains 10 mg PNS per each tablet. The blood serum samples were provided after three days of tablets administration and centrifuged at 1000 rpm for 12 minutes. The resulting supernatants were collected and used to prepare 0.1M PBS (pH 7.0) which were utilized as real samples. The amperometric measurements were applied to determine the PNS level in serum samples using MIP/Au@CNTs/GCE in prepared real samples from serum samples at -0.95V . The enzyme-linked immunosorbent assay kit (ELISA, LS-F27799, absorbance of 450nm , detection range from 5 to 100ng/ml , LSBio, Washington, USA) was also used for analyses of PNS level in blood serum samples.

The morphologies and microstructures of modified electrodes were characterized by the X-ray diffraction (XRD) and scanning electron microscopy (SEM).

3. RESULTS AND DISCUSSION

Fig. 1 indicates the morphologies of the surface of CNTs/GCE and MIP/ Au@CNTs/GCE. As observed from the SEM image of CNTs/GCE (Figure 1a), the electrodeposited CNTs formed the network with bundles with about 45 nm in diameter which adhered to each other to create a porous structure. The SEM image of MIP/Au@CNTs/GCE in Figure 1c exhibits a porous structure, confirming the electropolymerization MIP and removal of 2-oxindole template from the body of the polymer network.

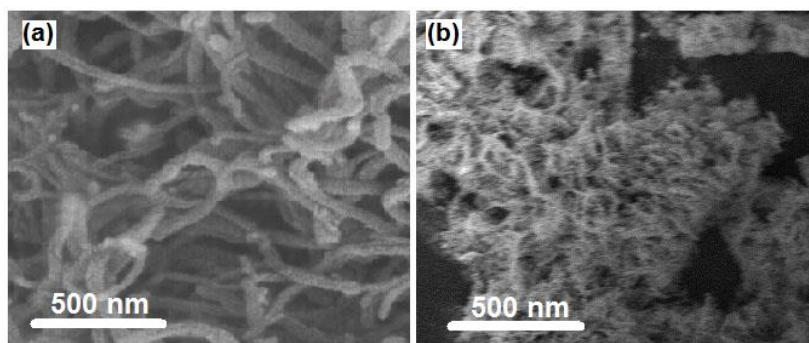


Figure 1. Surface morphologies of (a) CNTs/GCE, (b) MIP/Au@CNTs/GCE

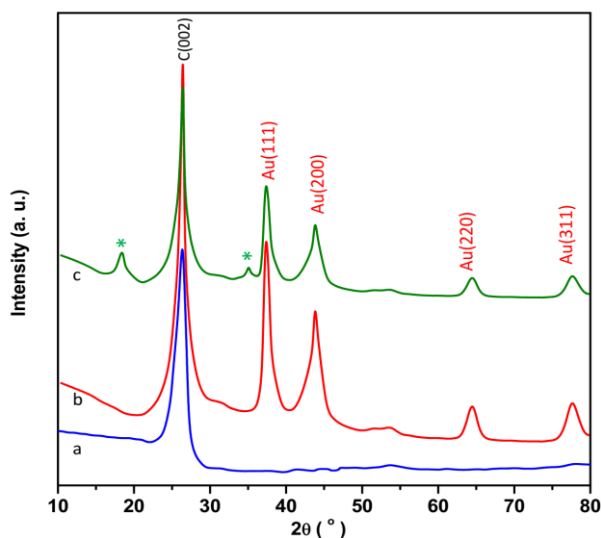


Figure 2. XRD pattern of (a)CNTs, (b) Au@CNTs and (c) MIP/Au@CNTs on GCE surface

Fig. 2 depicts the XRD pattern of CNTs, Au@CNTs and MIP/Au@CNTs on GCE surface. From Figure 2a, the XRD pattern of CNTs shows the strong peak at $2\theta = 26.21^\circ$ which is attributed to the plane (002) of graphitic carbon atoms. As indicated in Figure 2b, XRD pattern of Au@CNTs shows the (002) graphitic plane of CNTs, and diffraction peaks at $2\theta = 37.42^\circ$, 43.87° , 64.42° , 77.72° which related to (111), (200), (220), and (311) planes of the face-centered cubic (fcc) structure of Au nanoparticles (JCPDS card no. 04-0784), confirming the electrodeposition of Au@CNTs nanocomposite on GCE. XRD pattern of MIP/Au@CNTs in Fig. 2c shows the additional peaks at $2\theta = 18.38^\circ$ and 34.98° (marked with (*)), indicating the pattern of the loaded MIP matrix [28].

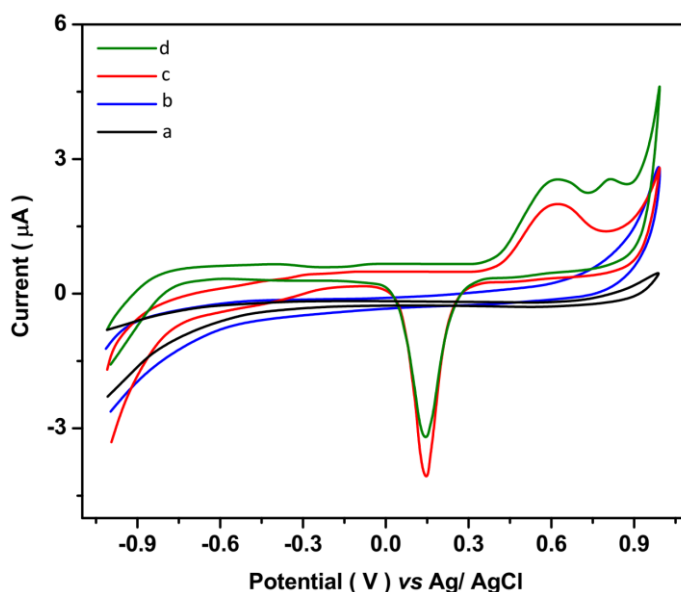


Figure 3. CV curves of GCE, CNTs/GCE, Au@CNTs/GCE and MIP/Au@CNTs/GCE in 0.1M PBS (pH/7.0) at 20mV/s scan rate in potential range from -1.0 to 1.0V

Figure 3 shows the CV curves of GCE, CNTs/GCE, Au@CNTs/GCE and MIP/Au@CNTs/GCE in 0.1M PBS (pH 7.0) at 20mV/s scan rate in potential range from -1.0 to 1.0V. As seen, the CV curves of GCE, CNTs/GCE do not show any redox peak, and Au@CNTs/GCE shows the redox peak at 0.62 V and 0.14 V, indicating to oxidation Au^0 into Au^+ and reduction of Au^+ to Au^0 [29-31], respectively. The CV curves of MIP/Au@CNTs/GCE show the redox peak of Au and additional oxidation peak of ρ -ATP at 0.81V [32, 33].

Figure 4 shows the DPV curves of GCE, CNTs/GCE, Au@CNTs/GCE and MIP/Au@CNTs/GCE in 0.1M PBS at a scan rate of 20mV/s in absence and presence of $8\mu\text{M}$ PNS in potential range from -1.25 to 0.2V. As seen before the addition $8\mu\text{M}$ PNS, the DPV curves of GCE (Figure 4a), CNTs/GCE (Figure 4b), Au@CNTs/GCE (Figure 4c) and MIP/Au@CNTs/GCE (Figure 4d) don't show any redox peak. After addition $50\mu\text{M}$ PNS in the electrochemical cell, the anodic peak was observed at -0.95V which related to reduction of PNS [22]. The available sites for reduction in prednisolone are the keto groups at position 3 which have a carbonyl group conjugated with a double bond that gives corresponding hydroxyl groups in a 2H^+ , 2e^- reaction [21, 22]. Comparison between DPV curves of electrodes reveals that the MIP/Au@CNTs/GCE (Figure 4d') shows the higher electrocatalytic current, indicating to sensitive response due to the synergic catalytic effect of MIP and Au@CNTs nanocomposite. Au@CNTs nanocomposite have remarkable effect for enhancing the sensitivity of MIP based sensors because of great specific surface area, good catalytic performance and high conductivity of CNTs and Au nanostructures which provide rapid mass transfer [34]. Moreover, comparison between the CNTs/GCE (Figure 4b'), Au@CNTs/GCE (Figure 4c') shows that Au nanostructures improve the catalytic activity and combination of Au nanoparticles and CNTs has created a new class of hybrid nanomaterials with efficient ionic diffusion, which resulted in increased charge transfer due to formation of spherical diffusion zones around the modified electrodes [35].

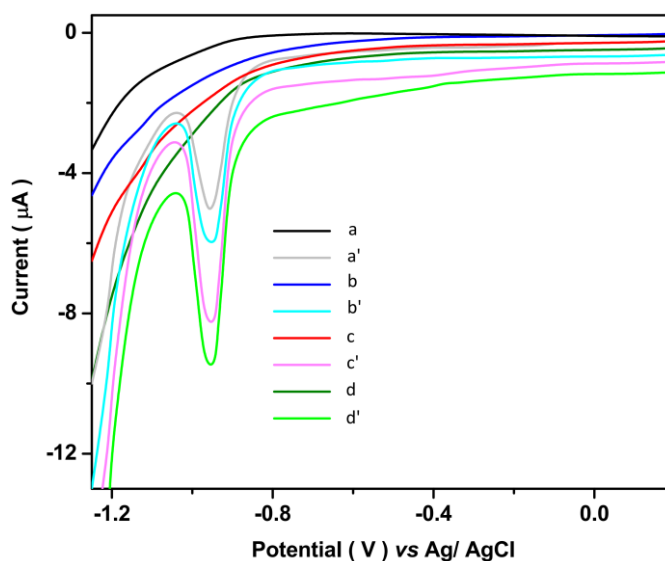


Figure 4. DPV curves of (a and a') GCE, (b and b') CNTs/GCE, (c and c') Au@CNTs/GCE and (d and d') MIP/Au@CNTs/GCE in 0.1M PBS at a scan rate of 20mV/s in absence and presence of $8\mu\text{M}$ PNS in potential range from -1.25 to 0.2V.

Further study was conducted for evaluation of the stability of response of electrodes towards the addition PNS. Figure 5 depicts the first and 50th DPV curves of GCE, CNTs/GCE, Au@CNTs/GCE and MIP/Au@CNTs/GCE into 0.1M PBS containing 8 μ M PNS at 20mV/s scan rate at potential range from -1.25 to 0.2V. As observed, the peak current density of electrodes at -0.95V is decreased after 50 continues scans. For GCE, CNTs/GCE, Au@CNTs/GCE and MIP/Au@CNTs/GCE is observed that the change in peak current after 50 continues scans is 24%, 13%, 14% and 3%, respectively, illustrating to the higher stability of electrochemical responses of MIP/Au@CNTs/GCE because of combination of ρ -ATP molecules with very stable nanocomposite of CNTs and Au nanoparticles. MIP as synthetic molecular recognition material have good structure design ability, high mechanical and chemical stability [36], and the porous structure of polymer possesses a precise placement of functional groups and a large number of binding sites on the surface of the modified electrode [37]. In addition, during the electropolymerization the self-assembled monolayer of ρ -ATP molecules created on the CNTs and Au nanoparticles by thiol groups which indicated to the great stability [38, 39]. Therefore, MIP/Au@CNTs/GCE as a highly sensitive and stable modified electrode was used for following electrochemical studies on PNS.

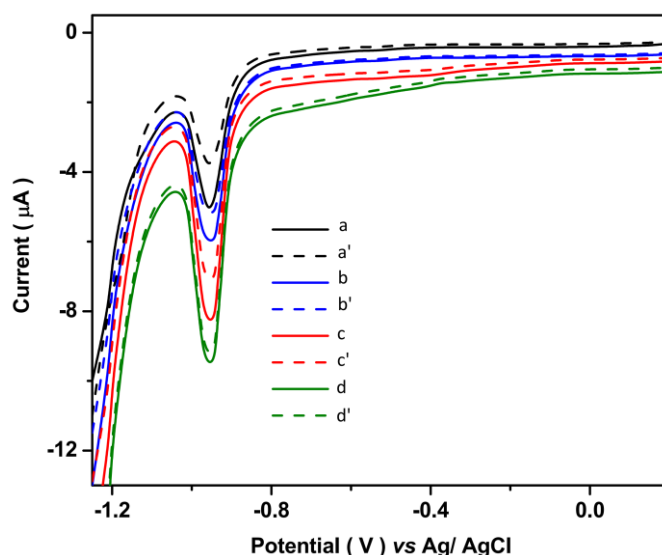


Figure 5. First (solid line) and 50th (dashed line) DPV plots of (a and a') GCE, (b and b') CNTs/GCE, (c and c') Au@CNTs/GCE and (d and d') MIP/Au@CNTs/GCE in 0.1M PBS (pH 7.0) containing 8 μ M PNS at a scan rate of 20mV/s in potential range from -1.25 to 0.2V.

Figure 6 displays the amperometric response and resulted calibration plot of MIP/Au@CNTs/GCE to successive injection of 15 μ M PNS solution into 0.1M PBS at -0.95V. It can be observed that the amperometric current is linearly improved with successive injection of PNS in electrochemical cell. The detection limit, sensitivity and linear range of the proposed sensor are found to be 0.003 μ M, 0.86207 μ A/ μ M and 1-210 μ M, respectively. These sensing properties were compared by the reported PNS sensors in literatures in Table 1, demonstrating a wide linear range and a lower

detection limit of MIP/Au@CNTs/GCE as PNS sensor that is attributed to the synergistic catalytic effect of MIP and Au@CNTs nanocomposite. The CNTs and Au nanoparticles enhance the sensitivity due to the excellent conductivity and large specific surface area [40]. MIP film electropolymerized on nanocomposite film and well adheres to the transducer surface. The ρ -ATP as a functional monomer strongly interacts with the nanocomposite and forms stable host–guest complexes [32, 41].

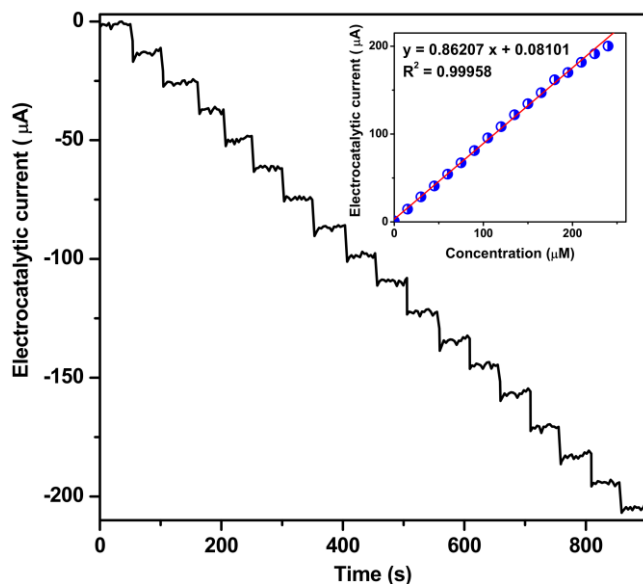


Figure 6. Amperometric measurement and resulted calibration plot of MIP/Au@CNTs/GCE to successive injection of 15 μ M PNS solution in 0.1M PBS (pH 7.0) at -0.95V.

Table 1. Comparing between the sensing properties of MIP/Au@CNTs/GCE with the reported PNS sensors in literatures

Electrodes	Technique	Detection limit (nM)	Linear range (μ M)	Ref.
MIP/Au@CNTs/GCE	AMP	3	1 to 210	This work
Ordered mesoporous carbon /GCE	SWV	57	0.06 to 40	[21]
SWNTs/edge plane pyrolytic graphite electrode	OSWV	9	0.01 to 100	[22]
GCE	OSWV	34	1 to 20	[23]
poly(4-vinylpyridine)/MIP/GO/GCE	DPV	4	1 to 120	[42]
Silica-coated paper /Screen-printed electrode	DPV	33236	27.77 to 138.88	[43]
Mercury film silver based electrode	DPAdSV	10	0.052 to 25	[44]
Hanging mercury drop electrode	DPAdSV	11	0.02 to 0.4	[45]
TSK-gel ODS-120T column	LC-UV	8.3	0.01 to 2.21	[16]
Phenyl-hexyl column	RP-HPLC	27.7	0.002 to 277	[15]

AMP: Amperometry; SWV: Square wave voltammetry; OSWV: Osteryoung square-wave voltammetry; DPAdSV: Differential-pulse adsorptive stripping voltammetric; LC-UV: liquid chromatography with UV detection; RP-HPLC: Reversed-phase high-performance liquid chromatography.

The selectivity of MIP/Au@CNTs/GCE as PNS sensor was also studied in presents of several metabolic substances in body fluids and drugs as interfering agents using amperometry method in 0.1M PBS at -0.95V. Table 2 shows the obtained amperometric current after successive addition of 1 μ M PNS and 10 μ M interfering agents. Results show that the amperometric response of MIP/Au@CNTs/GCE to addition of PNS is meaningfully higher than that response of interfering agents, and interfering agents show ignorable electrocatalytic signals. Thus, the interfering agents in Table 2 don't interfere with determining PNS using MIP/Au@CNTs/GCE. The sensitivity of MIP/Au@CNTs/GCE is related to the effective recognition sites in the molecularly imprinted polymer film for a target molecule [46]. Furthermore, the conductivity of a molecularly imprinted sensor is improved by polymerization of conductive polymers on Au@CNTs nanocomposite which promote biocompatibility and electroactivity [47].

Table 2. The amperometric current of MIP/Au@CNTs/GCE into 0.1M PBS at -0.95V after successive addition of 1 μ M PNS and 10 μ M interfering agents

Electrodes	Added(μ M)	Electrocatalytic peak current response(μ A) at -0.95V	RSD(%)
Prednisolone	1	0.8611	\pm 0.0107
Ascorbic Acid	10	0.0312	\pm 0.0010
Uric Acid	10	0.0108	\pm 0.0011
Acetaminophen	10	0.0202	\pm 0.0009
Xanthine	10	0.0325	\pm 0.0021
Chlordiazepoxide	10	0.0101	\pm 0.0010
Albumin	10	0.0441	\pm 0.0025
Diazepam	10	0.0620	\pm 0.0041
Hypoxanthine	10	0.0328	\pm 0.0022
Metolazone	10	0.0282	\pm 0.0010
Glucose	10	0.0173	\pm 0.0009
Naproxen	10	0.0187	\pm 0.0013
Nitrite	10	0.0229	\pm 0.0008
Ephedrine	10	0.0207	\pm 0.0008
Dopamine	10	0.0152	\pm 0.0007

The validity and accuracy of MIP/Au@CNTs/GCE to determine PNS were examined in prepared specimens of blood serum 5 young athletes aged 19 to 23 years who used PNS tablets. Table 3 shows the results of determinations of PNS for each sample through the amperometry and ELISA techniques. The comparison between the achieved results indicate good precision (RSD less than 4.15%) and good agreement between the ELISA and amperometry measurement on MIP/Au@CNTs/GCE. The results reveal that MIP/Au@CNTs/GCE as reliable PNS sensor may be used to monitor PNS level in blood serum of athletes.

Table 4. Results of determinations of PNS level using amperometry and ELISA techniques in prepared specimens of blood serum of young athletes aged 19 to 23 years who used PNS tablet.

Sample	PNS level in prepared samples of blood serum (ng/ml)			
	Amperometry		ELISA	
	MIP/Au@CNTs/GCE	RSD (%)	ELISA	RSD (%)
S1	5.08	±3.11	5.32	±3.21
S2	6.13	±3.29	6.21	±4.23
S3	5.94	±4.15	6.05	±3.95
S4	6.21	±4.03	6.17	±3.81
S5	6.03	±3.92	5.89	±3.71

4. CONCLUSION

This work was done on electrochemical study of MIP/Au@CNTs/GCE for detection of PNS as a sports doping agent. For synthesis of the sensor, the Au@CNTs nanocomposite was electrodeposited on GCE surface, and ρ -ATP and TBAP were electropolymerized on Au@CNTs/GCE. Results of SEM and XRD analyses revealed that those Au NPs were homogeneously deposited on a porous network of CNTs in Au@CNTs nanocomposite, and MIP was successfully electropolymerized on Au@CNTs/GCE. Results of electrochemical analyses indicated to stable, sensitive and selective performance of MIP/Au@CNTs/GCE to determination PNS, and the detection limit, sensitivity and linear range of proposed sensor were attained of $0.003\mu\text{M}$, $0.86207\mu\text{A}/\mu\text{M}$ and $1\text{-}210\mu\text{M}$, respectively. Comparing the sensing properties of MIP/Au@CNTs/GCE with the reported PNS sensors in literature demonstrated a wide linear range and lower detection limit of MIP/Au@CNTs/GCE. The validity and accuracy of MIP/Au@CNTs/GCE to determination of PNS were examined in prepared samples of blood serum 5 young volunteers who used PNS tablet and the results of determinations of PNS for each sample through the amperometry and ELISA techniques indicate good precision and agreement between the ELISA and amperometry measurement on MIP/Au@CNTs/GCE. Therefore, MIP/Au@CNTs/GCE as a reliable PNS sensor may be used to monitor PNS level in blood serum of athletes.

References

1. L. Liu, X. Zhang, Q. Zhu, K. Li, Y. Lu, X. Zhou and T. Guo, *Light: Science & Applications*, 10 (2021) 1.
2. H. Karimi-Maleh, Y. Orooji, F. Karimi, M. Alizadeh, M. Baghayeri, J. Rouhi, S. Tajik, H. Beitollahi, S. Agarwal and V.K. Gupta, *Biosensors and Bioelectronics*, 184 (2021) 113252.
3. P.S. Hench, C.H. Slocumb, H.F. Polley and E.C. Kendall, *Journal of the American Medical Association*, 144 (1950) 1327.
4. M. Shi, F. Wang, P. Lan, Y. Zhang, M. Zhang, Y. Yan and Y. Liu, *LWT*, 138 (2021) 110677.
5. M. Kadmiel and J.A. Cidlowski, *Trends in pharmacological sciences*, 34 (2013) 518.
6. Y. Yan, L. Feng, M. Shi, C. Cui and Y. Liu, *Food chemistry*, 306 (2020) 125589.

7. X. Zhang, Y. Tang, F. Zhang and C.S. Lee, *Advanced Energy Materials*, 6 (2016)
8. Y. Yang, J. Liu and X. Zhou, *Biosensors and Bioelectronics*, 190 (2021) 113418.
9. Z. Zhang, R. Xun, L. Wang and Z. Meng, *Ceramics International*, 47 (2021) 662.
10. J. Yan, Y. Meng, X. Yang, X. Luo and X. Guan, *IEEE Transactions on Information Forensics and Security*, 16 (2020) 1880.
11. X. Zhang, X. Sun, T. Lv, L. Weng, M. Chi, J. Shi and S. Zhang, *Journal of Materials Science: Materials in Electronics*, 31 (2020) 13344.
12. M. Wang, C. Jiang, S. Zhang, X. Song, Y. Tang and H.-M. Cheng, *Nature chemistry*, 10 (2018) 667.
13. M. Duclos, *The Physician and sportsmedicine*, 38 (2010) 121.
14. Y. Orooji, B. Tanhaei, A. Ayati, S.H. Tabrizi, M. Alizadeh, F.F. Bamoharram, F. Karimi, S. Salmanpour, J. Rouhi and S. Afshar, *Chemosphere*, 281 (2021) 130795.
15. A.N.B. Fonte, M.P. Legró and Y.R. Céspedes, *Journal of Liquid Chromatography & Related Technologies*, 36 (2013) 213.
16. M. Yamaguchi, J. Ishida, T. Yoshitake and M. Nakamura, *Analytica chimica acta*, 242 (1991) 113.
17. H. Shibasaki, H. Nakayama, T. Furuta, Y. Kasuya, M. Tsuchiya, A. Soejima, A. Yamada and T. Nagasawa, *Journal of Chromatography B*, 870 (2008) 164.
18. E. Dési, Á. Kovács, Z. Palotai and A. Kende, *Microchemical Journal*, 89 (2008) 77.
19. S.B. Ebrahimi, D. Samanta, B.E. Partridge, C.D. Kusmierz, H.F. Cheng, A.A. Grigorescu, J.L. Chávez, P.A. Mirau and C.A. Mirkin, *Angewandte Chemie International Edition*, 60 (2021) 15260.
20. S. Mazurek and R. Szostak, *Journal of pharmaceutical and biomedical analysis*, 40 (2006) 1225.
21. A. Muniyentwali and L. Zhu, *Journal of The Electrochemical Society*, 162 (2015) H278.
22. R.N. Goyal and S. Bishnoi, *Talanta*, 79 (2009) 768.
23. S. Yilmaz, S. Skrzypek, Y. Dilgin, S. Yagmur and M. Coskun, *Current Analytical Chemistry*, 3 (2007) 41.
24. X. Ji, B. Peng, H. Ding, B. Cui, H. Nie and Y. Yan, *Food Reviews International*, (2021) 1.
25. X. Li, Q. Yu, X. Chen and Q. Zhang, *Journal of Magnesium and Alloys*, (2021)
26. C. Jayakumar, C.M. Magdalane, K. Kaviyarasu, M.A. Kulandainathan, B. Jeyaraj and M. Maaza, *Journal of nanoscience and nanotechnology*, 18 (2018) 4544.
27. W. Guo, F. Pi, H. Zhang, J. Sun, Y. Zhang and X. Sun, *Biosensors and Bioelectronics*, 98 (2017) 299.
28. T.S. Anirudhan and S. Alexander, *Journal of Chemical Technology & Biotechnology*, 88 (2013) 1847.
29. E.E. Elemike, D.C. Onwudiwe, O.E. Fayemi and T.L. Botha, *Applied Physics A*, 125 (2019) 1.
30. J. Wang, C. Liu and J. Hua, *International Journal of Electrochemical Science*, 16 (2021) 2.
31. L. Zhou, *International Journal of Electrochemical Science*, 16 (2021) 2.
32. Q. Wang, J. Ji, D. Jiang, Y. Wang, Y. Zhang and X. Sun, *Analytical Methods*, 6 (2014) 6452.
33. R. Sun, C. He, L. Fu, J. Huo, C. Zhao, X. Li, Y. Song and S. Wang, *Chinese Chemical Letters*, (2021)
34. L. Yang, B. Zhang, B. Xu, F. Zhao and B. Zeng, *Talanta*, 224 (2021) 121845.
35. S. Mehmood, R. Ciancio, E. Carlino and A.S. Bhatti, *International journal of nanomedicine*, 13 (2018) 2093.
36. T. Sajini, M. Gigimol and B. Mathew, *Materials today chemistry*, 11 (2019) 283.
37. F. Tan, L. Cong, X. Li, Q. Zhao, H. Zhao, X. Quan and J. Chen, *Sensors and Actuators B: Chemical*, 233 (2016) 599.
38. A. Üzer, Ş. Sağlam, Z. Can, E. Erçağ and R. Apak, *International journal of molecular sciences*, 17 (2016) 1253.

39. J. Hu, J. Shi, S. Li, Y. Qin, Z.-X. Guo, Y. Song and D. Zhu, *Chemical physics letters*, 401 (2005) 352.
40. H. Xu, J. Peng, M. Zhu and J. Liu, *International Journal of Electrochemical Science*, 12 (2017) 10642.
41. A. Mishra, S. Dhiman and S.J. George, *Angewandte Chemie International Edition*, 60 (2021) 2740.
42. Y. Li and Y. Xiong, *International Journal of Electrochemical Science*, 16 (2021) 2.
43. V. Primpray, O. Chailapakul, M. Tokeshi, T. Rojanarata and W. Laiwattanapaisal, *Analytica chimica acta*, 1078 (2019) 16.
44. J. Smajdor, R. Piech and B. Paczosa-Bator, *Electroanalysis*, 28 (2016) 394.
45. S.I. Zayed, *Acta Chimica Slovenica*, 58 (2011) 75.
46. A.J. Kadhem, G.J. Gentile and M.M. Fidalgo de Cortalezzi, *Molecules*, 26 (2021) 6233.
47. A. Nezhadali and G.A. Bonakdar, *Journal of food and drug analysis*, 27 (2019) 305.

© 2022 The Authors. Published by ESG (www.electrochemsci.org). This article is an open access article distributed under the terms and conditions of the Creative Commons Attribution license (<http://creativecommons.org/licenses/by/4.0/>).